

# Searching Higgs in Noncommutative Electroweak Model at Photon-Photon Collider

Chien Yu Chen<sup>1,\*</sup>

<sup>1</sup>*Department of Physics, National Tsing-Hua University, Hsinchu 300, Taiwan*

We discuss the process of Higgs boson production in  $\gamma\gamma$  collider in noncommutative spacetime and compare the results with large extra dimension in KK graviton channel. Summing all KK mode on IR brane, the affections are in the same order by comparing noncommutative model prediction. This process is completely forbidden in standard model by unitary condition and bosonic distribution. In noncommutative theory, the effect is induced by the coordinates noncommutable relation,  $[x^\mu, x^\nu] = i\theta^{\mu\nu}$ . Due to the constant background strength tensor does not contain any conserved quantum number, the efforts should be indicated into particle power spectrum. Particle mass spectrum is corrected by radiational and anisotropic surroundings.

PACS numbers: 11.10.Nx; 14.80.Bn; 12.60.Fr

## I. INTRODUCTION

In modern high energy collider physics, it is based on standard model prediction. The spontaneous symmetry breaking mechanics (SSB) is used to generate particle mass from Higgs mechanics background methods. The scalar particle, Higgs, has not been found in the present collider experiments yet. It is expected to search this particle in further LHC and ILC linear acceleration experiments.  $\gamma\gamma$  collider experiment [1] is playing an important role to generate a pure source of high energy gamma ray. The experiment parameters in more wider energy range spectrum than  $e^+e^-$  linear acceleration collider experiments by controlling electron polarization pole,  $P_e$ , and incoming laser circle polarization,  $P_{laser}$ . The maximum energy range is similar 80% than  $e^+e^-$  collider annihilation.

In this paper, we analysis  $\gamma\gamma \rightarrow H_0 H_0$  in noncommutative spacetime. Noncommutative geometry is to correct the spacetime on the background magnetic field. Lorentz is violated by a constant and uniformed background large scale magnetic and electric field. The background universe framework indicates an isolated direction to violate the boost and rotation invariant under Lorentz transformation. In general Lorentz group  $SO(1,3)$  symmetry, it is divided into  $O(1,1) \otimes SO(1,2)$  at an alternative choice of a different boost axis in background uniformed direction. The commutative relation generates a  $\theta_{\mu\nu}$  deformed term [2], such as a strength field tensor,

$$[\hat{x}^\mu, \hat{x}^\nu] = i\theta^{\mu\nu}. \quad (1)$$

Otherwise, it is  $CPT$  conserved theory in four dimension spacetime [3]. The  $CPT$  violated effect is to consider a 5D extension [4]. The anisotropic geometry can induce a parity violated effect<sup>1</sup>. Otherwise, due to noncommutative theory inherently contains dipole moment [5], charge violation is imposed in isotropic and

homogeneous background universe. In  $U(1)$  model, the first order theta deformed term induces an anomaly electric dipole moment,  $\mathcal{J} \cdot \mathcal{E}$ .  $CP$  violated effect is produced by assuming that background strength tensor is not a Lorentz symmetric product. On the background of Lorentz violation, parity is not conserved under the globe symmetry. However,  $CP$  symmetry is eventual not a conserved quantity.

Charge is simultaneously violated in noncommutative electroweak theory, since triple photon coupling is produced automatically.  $CP$  violation is unobservable on the process with triple gauge boson coupling. We cannot explore the time asymmetry effect from noncommutative spacetime structure with  $CPT$  symmetry. In standard model extension, scalar sector includes both  $CP$ -even,  $H_0$  and  $h_0$ , and  $CP$ -odd,  $A_0$ , particles [6, 7, 8, 9]. Those correspond to the terms  $(\vec{\epsilon}_1 \cdot \vec{\epsilon}_2)$  and  $(\vec{\epsilon}_1 \times \vec{\epsilon}_2) \cdot \vec{k}_\gamma$  respectively. In noncommutative geometry, the momentum of  $CP$ -even,  $H^0$ , Higgs boson couples to photon polarizations is,  $\vec{p}_1 \cdot \vec{\epsilon}_1$ . However,  $H^0$ , Higgs boson with total angular momentum,  $J=0$ , conserves parity symmetry.

The process of  $\gamma\gamma \rightarrow H_0 H_0$  is completely forbidden at tree level process, because the coupling,  $Z\gamma\gamma$ , cannot be predicted in standard model. It violates angular momentum conservation in loop order [10, 11]. Phenomenologically, it is produced under triple gauge boson condensation via Seiberg-Witten map [2, 11]. Therefore, significantly, zero total angular momentum,  $J=0$ , contributes at event point. Mediate gauge boson does not interact with background field by angular power overlap. The distribution is dominated by the product of background field to particle polarization with total angular momentum,  $J=0$ . It manifests that if we set electron polarization as same as laser photon,  $p_e = 1$  and  $p_l = -1$ , on the event point. The total photon luminosity will be maximum contributed. Contrastively, if we choose electron and incoming laser zero polarized pole, the contribution on the cross section only contains the minimal strength of event. We discuss the influence by comparing with each electron and laser photon polarization,  $p_e$  and  $p_l$ . Finally, in photon power spectrum, high energy phenomena is poor to redistribute by exchanging the central energy range. At the central energy lower than 500 GeV, the change is dramatically independent with particle mass distribution.

\*Electronic address: [d9522817@phys.nthu.edu.tw](mailto:d9522817@phys.nthu.edu.tw)

<sup>1</sup> Isotropic spacetime geometry conserves angular distribution and energy power spectrum by alternative coordinate translation. On the cosmic uniformed background field, we choose a frame to violate the coordinate translational invariance. In the background preferred frame, the effects induced by the remanent field is unobservable.

## II. NONCOMMUTATIVE HIGGS SECTOR

Higgs sector is a scalar field dominating particle mass, and contains all of the symmetry,  $SU_L(N) \otimes SU_R(N) \rightarrow SU_V(N)$  in quantum field theory. Noncommutative theory is a perturbative theory coming from string theory without considering the exotic field. The general statistic quantum field situation is still considered. Following the discussion of  $CPT$  symmetry, the field average out of the equilibrium is disappeared in the restriction of  $CP$  or  $CPT$  conservation. Noncommutative theory generally describes a symmetry, *Panchar* transformation, on the alternative expansion of  $\theta$  deformation. The boost effect does not produce a modification of particle statistical properties in global system. Scalar field is working on universe equilibrium, no  $CPT$  violated effect can be observed, such as baryogenesis and leptogenesis [12]. Otherwise, vector potential, spin-1, and graviton, spin-2, are bosonic fields, the angular momentum polarized spectrum interacts with background field and generate different mode on the anisotropic spacetime background. In [13, 14], absorbing the  $\theta$  deformed term into graviton field, and assuming that the geometric fluctuation is composed by the tensor field,  $\theta_{\mu\nu}$ ,

$$\begin{aligned} h^{\mu\nu} &= \theta^{\mu\alpha} F_\alpha^\nu + \theta^{\nu\alpha} F_\alpha^\mu + \frac{1}{2} \eta^{\mu\nu} \theta^{\alpha\beta} F_{\alpha\beta}, \\ h &= 0, \end{aligned} \quad (2)$$

and [15] deforms spacetime coordinate on the module expansion,  $\hat{x}^\mu = x^\mu + \theta^{\mu\nu} \partial_\nu f(x)$ . In addition, some papers consider nonsymmetric matrix to model a noncommutative geometry [16], and discuss a nonsymmetric graviton on annihilation collider event [17]. Modifying spin background is equal to redefine the angular power spectrum and particle mass distribution. Mapping gauge boson to noncommutative spacetime by Seiberg-Witten map

$$\hat{V}_\mu = V_\mu + \frac{1}{4} \theta^{\alpha\beta} \{ \partial_\alpha V_\mu + F_{\alpha\mu}, V_\beta \} + \mathcal{O}(\theta^2), \quad (3)$$

where noncommutative deformed vector potential is constructed by standard model field and the  $\theta_{\mu\nu}$  deformed term. In general gauge potential on the non-abelian group, U(1) quantum number is constrained by the relation,  $Q = T_3 + Y$ ,  $Y$  is hypercharge and  $T_3$  is nonabelian traceless eigenvalues. The general expres-

sion is

$$V_\mu = g' A_\mu Y + g \sum_{i=1}^3 B_\mu^i T_L^i + g_S \sum_{i=1}^8 G_\mu^i T_S^i, \quad (4)$$

extended by U(1) and non-abelian gauge group generator. Splitting U(1) gauge potential into two part, contains both hypercharge  $Y = \frac{1}{2}$  with different gauge couplings. In unitary gauge, Higgs field is rotated to

$$\hat{\Phi} = \begin{pmatrix} \hat{\Phi}^+ \\ \hat{\Phi}^0 \end{pmatrix}, \quad (5)$$

charged Higgs should be forbidden by choosing unitary transformation. It preserves the neutral Higgs on vacuum and a constant shift  $v$  by SSB breaking scalar potential.

In NC electroweak model [10], Higgs field is under the fundamental and anti-fundamental transformation, due to Yukawa term couples to the left-handed fermion and right-handed fermion under different representation of  $SU_L(2)$  and  $U_Y(1)$ . The expression on noncommutative deformed representation is described as

$$\begin{aligned} S_{Higgs} &= \int d^4 \left\{ \frac{1}{2} (\hat{D}_\mu \hat{\Phi})^\dagger \star (\hat{D}^\mu \hat{\Phi}) - \frac{\mu^2}{2!} \hat{\Phi}^\dagger \star \hat{\Phi} \right. \\ &\quad \left. - \frac{\lambda}{4!} \hat{\Phi}^\dagger \star \hat{\Phi} \star \hat{\Phi}^\dagger \star \hat{\Phi} \right\}, \end{aligned} \quad (6)$$

the general expression of scalar field and its covariant derivative are

$$\begin{aligned} \hat{\Phi} &= \Phi + \frac{1}{2} \theta^{\alpha\beta} V_\beta^m D_\alpha^\Phi \Phi, \quad D_\alpha^\Phi = \partial_\alpha - i V_\alpha^\Phi, \\ \hat{D}_\mu \hat{\Phi} &= \partial_\mu \hat{\Phi} - i [\hat{V}_\mu^{-\frac{1}{2}} \star \hat{\Phi} - \hat{\Phi} \star \hat{V}_\mu^{-1}] - i \hat{V}_\mu^{SU(2)} \star \hat{\Phi}, \end{aligned} \quad (7)$$

where  $\hat{V}_\mu^{-\frac{1}{2}}$  and  $\hat{V}_\mu^{-1}$  are vector fields, Eq.(2), the hypercharge are  $-\frac{1}{2}$ , and  $-1$ . The general expression of gauge potential for above terms is splitting gauge boson into hypercharge  $Y = -\frac{1}{2}$ ,  $-1$ , and non-abelian term. Vector field overlaps with Higgs field region will generate a mass distribution. On the other hand, particle mass is dominated with the area coupled by Higgs field. Photon couples to Higgs field should generate a region producing an overlap with scalar vacuum.

$$\begin{aligned} \hat{V}_\mu^\Phi &= \hat{V}^{-\frac{1}{2}} - \hat{V}^{-1} + \hat{V}_\mu^{SU(2)} = \begin{pmatrix} e\hat{A}_\mu + e \cot 2\theta_W \hat{Z}_\mu^0 & \frac{e}{\sqrt{2} \sin \theta_W} \hat{W}_\mu^+ \\ \frac{e}{\sqrt{2} \sin \theta_W} \hat{W}_\mu^- & -\sin 2\theta_W \hat{Z}_\mu^0 \end{pmatrix} \\ \hat{V}_\mu^m &= \hat{V}^{-\frac{1}{2}} + \hat{V}^{-1} + \hat{V}_\mu^{SU(2)} = \begin{pmatrix} -e\hat{A}_\mu + \frac{e}{2} (3 \tan \theta_W + \cot \theta_W) \hat{Z}_\mu^0 & \frac{e}{\sqrt{2} \sin \theta_W} \hat{W}_\mu^+ \\ \frac{e}{\sqrt{2} \sin \theta_W} \hat{W}_\mu^- & -e\hat{A}_\mu + \frac{e}{2} (3 \tan \theta_W - \cot \theta_W) \hat{Z}_\mu^0 \end{pmatrix} \end{aligned} \quad (8)$$

The mixture part devotes on the coupling of one gauge boson to Higgs field. On this process, we extract the

coupling of photon and  $Z^0$  to two Higgs. Testing photon-photon collider experiments, we get a consis-

tent signature in cosmology background field direction. Following, [10], we rewrite the Higgs sector after correcting the gauge potential. Splitting gauge field into standard and vector field, including  $Y=-1$  and  $Y=-\frac{1}{2}$  respectively. The couplings to neutral Higgs will be split either.

In order to put a constraint on U(1) gauge,  $Q = T_3 + Y$ , the coupling constant on  $A_\mu$  and  $Z_\mu^0$  gauge field is modified. Photon and  $Z_\mu^0$  U(1) gauge boson are the same kind field on the second term in Eq.(7).  $Z_\mu^0$  is a massive particle, photon and neutral  $Z_\mu^0$  gauge boson with the same generator will induce a clue, photon mixes with  $Z_\mu^0$  field by translating the splitting to different coupling constant. Using enveloping algebra to expand gauge sector, the phenomena is presented. In noncommutative spacetime structure, the mixture term induces a forbidden couplings, Fig.(1), and modifies the relation between neutral Higgs and U(1) gauge boson angular distribution on 4D brane.

In Eq.(7),  $Z_\mu^0$  gauge boson mixes with photon, the general expression of Higgs sector is

$$\begin{aligned}
S_{Higgs} = & \frac{1}{2} \int d^4x [(D_\mu^\Phi \Phi)^\dagger (D_\mu^\Phi \Phi) - \mu^2 |\Phi|^2 - \lambda |\Phi|^4] \\
& + \frac{\theta^{\alpha\beta}}{4} \int d^4x \Phi^\dagger \left\{ U_{\alpha\beta} + U_{\alpha\beta}^\dagger + \frac{\mu^2}{2} F_{\alpha\beta}^m \right. \\
& - i \frac{\lambda}{12} \Phi [(\partial_\alpha \Phi)^\dagger D_\beta^m + i \Phi^\dagger V_\alpha^m D_\beta^\Phi] \\
& - i \frac{\lambda}{12} \Phi [(\partial_\alpha \Phi)^\dagger \partial_\beta - i (D_\alpha^\Phi \Phi)^\dagger V_\beta^m] \\
& \left. - i \frac{\lambda}{12} \Phi \Phi^\dagger [V_\alpha^\Phi V_\beta^m + V_\beta^m V_\alpha^\Phi] \right\} \Phi,
\end{aligned} \tag{9}$$

where  $F_{\alpha\beta}^m$  is Maxwell term by considering,  $V_\mu^m$ , the gauge potential and the tensor field,  $U_{\alpha\beta}$ . The tensor field form is as follows

$$\begin{aligned}
U_{\alpha\beta} = & (\overleftarrow{\partial}^\mu + iV^{\Phi\mu}) \left[ -(\partial_\mu V_\alpha^m) \partial_\beta - V_\alpha^m \partial_\mu \partial_\beta + (\partial_\alpha V_\mu^m) \partial_\beta \right. \\
& + iV_\alpha^m (\partial_\mu V_\beta^\Phi) + iV_\alpha^m V_\beta^\Phi \partial_\mu + iV_\mu^\Phi V_\alpha^m \partial_\beta + i(\partial_\mu V_\alpha^m) V_\beta^\Phi \\
& \left. + \frac{i}{2} \{V_\alpha^\Phi, \partial_\beta V_\mu^\Phi + F_{\beta\mu}^\Phi\} + V_\mu^\Phi V_\alpha^m V_\beta^\Phi \right],
\end{aligned} \tag{10}$$

where  $F_{\beta\mu}^\Phi$  is taking  $V_\mu^\Phi$  potential into consideration. Using Eq.(6) and Eq.(7) in Higgs sector, we can get the feymann rules, Fig.(1), on complete  $\theta_{\mu\nu}$  deformed coupling constant. The quantity is associated with the background field direction and the incoming particle energy.

On the background surroundings, the deformed magnetic and electric field will produce a discrete patch to modify quantum field theory. The interaction with the other fields by coupling to background  $\theta_{\mu\nu}$  perturbative term, and those efforts are coming from the overlap with large scale magnetic field. Therefore, in this paper, we focus on the discussion with the coupling between Higgs field and U(1) gauge boson by considering the process of high energy gamma ray to two neutral Higgs particles.

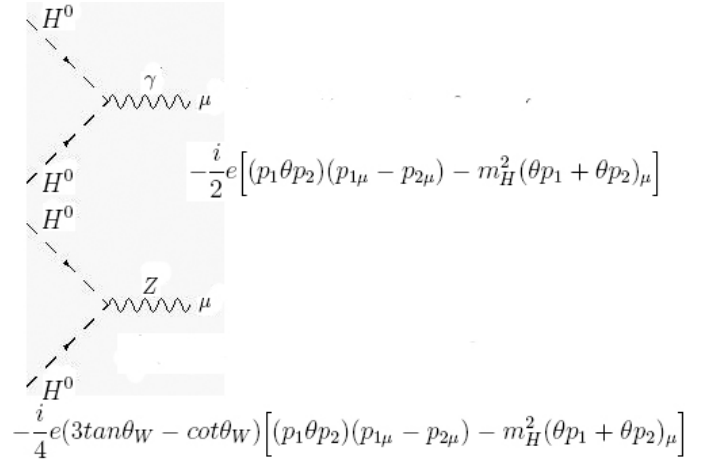


FIG. 1: The couplings of neutral Higgs to two chargeless gauge bosons. These couplings are completely forbidden by standard model prediction.

### III. PHOTON COLLIDER EXPERIMENTS

On the next linear collider, it is in order to search Higgs particle, superpartner, and towards to explore the Planck scale physics at TeV energy level. Large Hardron Collider (LHC), International Large Collider(ILC), and photon collider experiment (TESLA), etc.. In this paper we work in probing Higgs particle at pure source photon-photon collider experiments data analysis. The photon collider at TESLA is using two observable technology methods to generate pure gamma ray. First is  $\gamma\gamma$  technique methods, by considering polarized electric beam,  $p_e$ , interfered with polarized high energy gamma ray,  $p_l$  [1] at electron bunch point. The other is  $\gamma e$  photon collider into electron target. The total incoming photon luminosity,  $L_{\gamma\gamma}$ , is around  $\frac{1}{3}L_{e^+e^-}$  electron beam producing. The background of photon collider is in the polarized electron beam at electron bunch point. We rearrange incoming electron beam by setting the polarized parameter  $p_e = 0$  or  $1$  for unpolarized and polarized channel, and  $p_\gamma = -1, 0, 1$  for interacted channel.

Different polarized electron and laser photon beam will produce a different incident source by backreact scattering effects. The energy scale at 800 GeV, photon luminosity approaches to  $1.7 (cm^{-2} \cdot s^{-1})$  magnitude, electron luminosity is around 5.8 unit. By considering the polarized electron beam and photon beam, we have to take photon polarization distribution function,  $\xi(x)$ , into account. The result is under multiplying fractional luminosity and integrating the energy rate, x and y. The central energy is  $\sqrt{s} = E_{CM}$ ,  $E_{CM} = xE_1 + yE_2$ , it constrains laser energy range in  $x + y = 1$  on the incident point by energy conservation condition. The integration range is decided by creating mediator particle and the kinetic momentum of final state particle. The final particle kinetic energy has to be positive, and the fractional energy range truncates on the branch  $\frac{M_Z}{\sqrt{s}}$ .

The spin-1 particle contains 3 polarized state, spin up, spin-0, and spin down. The positive channel is canceled out by opposite sign, due to helicity conservation

condition. The zero channel is parity conserved without exotic background influence. The zero polarized cross section can be written as

$$\sigma_C = \frac{v}{s} \left( \frac{\alpha}{2} \right)^2 \int^{x_m} d\Omega |M_{J_z=0}|^2 \quad (11)$$

$$|M_{J_z=0}|^2 = \frac{|M_{++}|^2 + |M_{--}|^2}{2},$$

in which,  $v$  is the velocity of final state particle,  $\alpha$  is fine structure constant, and  $x_m \approx 2(+\sqrt{2})$  is maximum energy fractional rate in photon collider. The luminosity amplitude in photon collider background is

$$\sigma_L = \int dx dy f(x) f(y) \left( \frac{1 + \xi(x)\xi(y)}{2} \right) \sigma_C, \quad (12)$$

by integrating out the parameter  $x$  and  $y$ , the fractional energy of incident laser photon, and  $v$  is velocity of the outgoing massive particle. Under the condition of parity conservation, each incoming laser photon cross section is consistent with different final helicity state, the "+" and "-" denote different circle polarization. In [18], it considers radion particle field in Randall-Sundrum model at photon collider experiment.

In next section we briefly introduce the Higgs generation process on large extra dimension model. The devotion is very small by comparing noncommutative process. We use the discussed polarized luminosity function in [18]

$$f(x) = \frac{dL_{\gamma\gamma}}{dz} \frac{1}{L_{geom}} \quad (13)$$

where

$$L_{geom} = \left[ \left( 1 - \frac{4}{z} - \frac{8}{z^2} \right) \ln(z+1) + \frac{1}{2} + \frac{8}{z} - \frac{1}{z(z+1)^2} \right] + p_e p_l \left[ \left( 1 + \frac{2}{z} \right) \ln(z+1) - \frac{5}{2} + \frac{1}{z+1} - \frac{1}{2(z+1)^2} \right] \quad (14)$$

and

$$\frac{dL_{\gamma\gamma}}{dz} = \frac{1}{1-x} + (1-x) - 4r(1-r) - p_e p_l r z (2r-1)(2-x). \quad (15)$$

in the Higgs produced process. The polarization of initial state photon is associated with the electron and photon polarized beam,  $p_e$  and  $p_l$ ,

$$\xi(x) = \frac{1}{L_{geom}} \left\{ p_e \left[ \frac{x}{1-x} + x(2r-1)^2 \right] - p_l (2r-1) \left[ 1-x + \frac{1}{1-x} \right] \right\}. \quad (16)$$

The photon polarized strength is dependent on incoming electron polarization and laser photon polarization. It generates the transverse and linear photon state by controlling the incoming electron and laser beam.

#### IV. LARGE EXTRA DIMENSION MODEL

Extra dimension is to extend our spacetime in  $4+n$  dimension in  $SO(1, n+3)$  group without modifying time component. There are two aspects to introduce extra dimension model. First, considering the polynomial expansion, the coordinate is added a five dimension coordinate variable,  $x^n = \frac{\vec{n} \cdot \vec{y}}{R}$  [19, 20]. In general, the geometry in extra dimension framework is written as,  $g^{\hat{\mu}\hat{\nu}}$ . The index  $\hat{\mu}$  and  $\hat{\nu}$  are in  $n+4$  dimensions, from 4 to extra  $4+n$ . The variable  $y$  is the fifth extra coordinate space, particle field can project to bulk in the radius  $R$ , and the extra extended spacetime,  $y$ , with KK mode expansion. The other is to consider the two p-brane world-sheet [21],  $p=3$ , on the warped bulk surroundings, one is IR visible brane, and another is UV invisible brane. The particle field can be separated into five dimension part and original four dimension field. Summing all influence on warped extra dimension by integrating out the 5D component  $y$ , we can get a exotic mixing between different particle field generation, such as flavor changing neutral current and neutrino mass [22].

In general consideration, particle field is survived on the 4D brane. For large extra dimension case, the extra 5 dimension produces a closed loop in the bulk space, from a 4D spacetime point to bulk field and coming back to the same point. This circle phenomena is enclosed in a box space containing bulk wave function. In this box, each wave function on the ending point is disappeared, the bulk space can produce a static wave. Each nodal point can be regarded as a cutting dot. The stored energy [23] and produced pressure [24] on the box surface is coming from the wave function dispersing into extra dimension. Summing over the devotion, particle field will be sinuously corrected. The mass term on bulk radius can be deduced by the d'Alembert operator. In graviton case,  $\square_{4+n}(\hat{h}^{\hat{\mu}\hat{\nu}} - \frac{1}{2}\eta_{\hat{\mu}\hat{\nu}}\hat{h}) = \hat{h}^{\hat{\mu}}_{\hat{\mu}} = 0$ , are produced onto graviton field. Then, after redefining, extracting the physical field, the bulk mass term will be produced by the form  $m_{\vec{n}}^2 = \frac{4\pi^2 \vec{n}^2}{R^2}$ . On 4D brane, graviton is massless,  $m_4 = m_{\vec{n}=0} = 0$ .

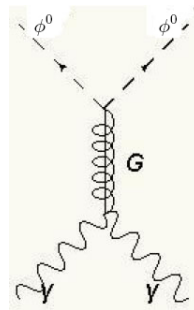


FIG. 2:  $\gamma\gamma \rightarrow Grav. \rightarrow \phi^0\phi^0$

Focusing on the graviton field [25], extending metric into extra dimension index. Graviton field is a geodesic fluctuation products. In five dimension spacetime, the extra space-like vector on the graviton field is emerged, and the other scalar component is also imposed in the geometry inflation. By considering the gauge condi-

TABLE I: Large extra dimension data analysis at  $E_{CM} = 800$  GeV, and on the string scale  $M_S = 1$  TeV

$\sigma_{pol.}^n / \sigma_{Unpol.}^n$	$p_e=1, p_l=-1$	$p_e=1, p_l=0$	$p_e=1, p_l=1$
n = 0	0.112538	0.055313	0.0207263
n = 2	0.465354	0.224496	0.0895319
n > 2	0.0620941/(n-2)	0.0319583/(n-2)	0.0152298/(n-2)

<sup>a</sup>The Higgs boson mass  $m_\phi$  at 150 GeV.

tion, assuming no background field in gravitational radiation region, graviton field is re-composed into the other physical situations. In this model, all the matter field is restricted in the 4D brane, only graviton field can project to five dimension spacetime. We discuss the phenomenon into probing Higgs field at the photon-photon collider experiments. By considering *Casimir effect*, the stored bulk energy is a curious point to take the incident into account. Using the feymann rule in [25], the total cross section in even dimension is listed in Tab.I.

The graviton amplitude is written as

$$M_{\gamma\gamma \rightarrow G \rightarrow \phi\phi} = -iD_n \left( \frac{k}{2} \right) \epsilon_1^\mu \epsilon_2^\nu \left( \frac{s}{2} c_{\mu\nu, \alpha\rho} + D_{\mu\nu, \alpha\rho} \right) B^{\alpha\rho, \beta\sigma} (m_\phi^2 \eta_{\beta\sigma} - c_{\beta\sigma, \xi\eta} k_1^\xi k_2^\eta), \quad (17)$$

where the tensor field  $C_{\rho\sigma, \xi\eta}$  and  $D_{\mu\nu, \alpha\rho}$  is the coupling tensor. The  $\frac{1}{2}B^{\alpha\rho, \beta\sigma}$  is graviton spin polarization sum in bulk spacetime with mass  $m_{\tilde{n}}$ . The  $D_n$  is graviton projector.

For n = 0 case,

$$D_0 = \frac{i}{s}. \quad (18)$$

For n = 2 case,

$$D_2 = -\frac{i}{4\pi} R^2 \text{Log} \left( \frac{M_S^2}{s} \right). \quad (19)$$

For n  $\geq 2$  case,

$$D_{\geq 2} = -\frac{2i}{(n-2)\Gamma(\frac{n}{2})} \frac{R^n M_S^{n-2}}{(4\pi)^{\frac{n}{2}}}. \quad (20)$$

The polarization rate are listed in the Tab.I. Due to extra dimension works on odd dimension bulk space. There is an anomaly problem will be generated on the odd order extra dimension number, n. In n = 2 case, six dimension spacetime, the polarized rate is maximum contributed on the Higgs creation process.

The radius  $R$ , cosmology constant and string effective scale  $M_S$  are redefined into the restriction  $\frac{1}{G_N} \approx M_S^{n+2} R^n$ . In the  $n$ th extra dimension devotion, the relation between gravitational constant  $\kappa$  and  $R^n$  is inside into a region  $16\pi(4\pi)^{\frac{n}{2}} \Gamma(\frac{n}{2}) M_S^{-(n+2)}$ . We take the mainly domain on the assumption of  $M_S \gg s$ . The bulk field in extra dimension box  $\frac{2\pi^{\frac{n+4}{2}}}{\Gamma(\frac{n+4}{2})} R^n$ . In excluding *Casimir effect*, the single graviton mode is similar order magnitude by considering the string effective scale,  $M_S$ .

## V. THE PROCESS OF $\gamma\gamma \rightarrow$ HIGGS

The nature source of high energy gamma ray collision is coming from sky. The process of gamma-gamma collision is a frequent incidence on the astroparticle physics. We test these phenomena by linear high energy photon-photon collider experiments, and model the cosmological incidents on large scale background. In the noncommutative spacetime, the background magnetic field and electric field will interact with particle spin and electric charge via  $\theta_{\mu\nu}$  connection. From Eq.(11), we clearly understand the background field how to product with the initial state photon polarization vector and interact with final charged fields. We analysis the particle power spectrum in the photon photon collider experiments. This dramatic field interaction induces a sensitive effect associative with the *Planck* scale  $\Lambda_c$  and the background direction on the final physical result.

The Tab.II lists the quantum numbers at Higgs particle internal symmetry. We use this discussed particle properties on the  $\gamma\gamma \rightarrow$  Higgs process. Otherwise, the Tab.III concerns the model restriction on the standard 2HDM and the supersymmetry 2HDM. The particle mass spectrum is defined by the two vacuum  $v_1$  and  $v_2$ , the axion mass is a free parameter in the model building, another is the vacuum fractional rate  $\tan \beta$ .

### A. $\gamma\gamma \rightarrow H^0 H^0$

In this section, we introduce the process and analyze the properties of polarized and unpolarized beam. Comparing the probability distribution and particle mass spectrum in the different field. The total cross section is maximum rearranged by background magnetic and electric field perpendicular to the incoming particle direction. The ratio of polarized and unpolarized beam under different polarization electron and incoming laser photon, we set the Higgs mass,  $m_{H^0} = 150$  GeV,  $m_{H^\pm} = 120$  GeV, and  $m_{A^0} = 100$  GeV. The central energy up to 800 GeV with the scale of  $\Lambda_c = 1$  TeV and the triple gauge boson coupling  $K_{ZZ\gamma\gamma} = -0.2$ ,  $K_{\gamma\gamma\gamma} = -0.3$ . There is a minimum devotion on the central energy around the region 100 GeV  $\sim$  500 GeV.

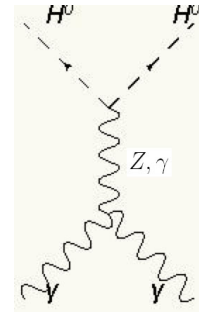


FIG. 3:  $\gamma\gamma \rightarrow z\gamma \rightarrow H_0 H_0$ .

The  $\gamma\gamma$  collider technology can be used to simulate cosmology high energy gamma ray annihilation phenomena. Background high energy frequency is produced by photon gas entropy. The gradient distribution is a

TABLE II: Quantum numbers of Higgs and Gauge Bosons

	$J^{PC}$		$J^P$
<b>When <math>C</math> and <math>P</math> are separately conserved</b>			
$\gamma$	$1^{--}$	$W^\pm$	$1^-$
$Z$	$1^{--}$	$H^\pm$	$0^+$
$H^0$	$0^{++}$		
$h^0$	$0^{++}$		
$A^0$	$0^{+-}$		
<b>When <math>C</math> and <math>P</math> are violated but <math>CP</math> still conserved</b>			
$\gamma$	$1^{--}$	$W^\pm$	$1^-, 1^+$
$Z$	$1^{--}, 0^{++}$	$H^\pm$	$0^+, 0^-$
$H^0$	$0^{++}, 0^{--}$		
$h^0$	$0^{++}, 0^{--}$		
$A^0$	$0^{+-}, 0^{-+}$		

<sup>a</sup>The table in pages 198, *The Higgs Hunter's Guide*

TABLE III: The experiments bounds on  $\tan\beta$  and scalar mass  $m_{H^0}$  and  $m_{H^\pm}$ 

	$\tan\beta$ and $m_{H^0}$
ACHARD 03C	$m_{H^0} > 108.1 \text{ GeV}$ . For $B(H^0 \rightarrow \gamma\gamma)=1$ , $m_{H^0} > 114 \text{ GeV}$ .
ABBIENDI 02D	$4 < m_{H^0} < 12 \text{ GeV}$
99E	For $B(H^0 \rightarrow \gamma\gamma)=1$ , $m_{H^0} > 117 \text{ GeV}$ .
ACCIARRA 00s	$m_{H^0} = m_{A^0}$ in general 2DHM. The limits on $\Gamma(H^0 \rightarrow \gamma\gamma) \cdot B(H^0 \rightarrow \gamma\gamma \text{ or } b\bar{b})$ for $m_{H^0} > 98 \text{ GeV}$
BARATE 00L	For $B(H^0 \rightarrow \gamma\gamma) = 1$ , $m_{H^0} > 98 \text{ GeV}$ .
ABBOTT 99B	For $B(H^0 \rightarrow \gamma\gamma) = 1$ , $m_{H^0} > 109 \text{ GeV}$ .
ALEXANDER 96H	Limits in the range of $\sigma(H^0 + Z/W) \cdot B(H^0 \rightarrow \gamma\gamma) = 0.80\text{-}0.34 \text{ pb}$ are obtained in $m_{H^0} = 65\text{-}150 \text{ GeV}$ . $B(Z \rightarrow H^0\gamma) \times B(H^0 \rightarrow q\bar{q}) < 1.4 \times 10^{-5}$ 95% CL and $B(Z \rightarrow H^0\gamma) \times B(H^0 \rightarrow b\bar{b}) < 0.7\text{-}2 \times 10^{-5}$ 95% CL in $20 < m_{H^0} < 80 \text{ GeV}$ .
	$\tan\beta$ and $m_{H^\pm}$
ABULENCIA 06E	Within MSSM, the region $\tan\beta < 1$ or $> 30$ in $m_{H^\pm} = 80\text{-}160 \text{ GeV}$ .
ABBIENDI 03	$m_{H^\pm} > 1.28 \tan\beta \text{ GeV}$ 95% CL in type II.
01Q	$\tan\beta < 0.53 m_{H^\pm} \text{ GeV}^{-1}$ 95% CL in type II.
ABAZOV 02B	$\tan\beta > 32.0$ excluded at 95%CL $m_{H^\pm} = 75 \text{ GeV}$ . The excluded mass region extends to over 140 GeV for $\tan\beta > 100$ .
BARATE 01E	$\tan\beta < 0.40 m_{H^\pm} \text{ GeV}^{-1}$ 90% CL in type II and $< 0.49 m_{H^\pm} \text{ GeV}^{-1}$ 90% CL.
AFFOLDER 001	For $\tan\beta > 100$ , $m_{H^\pm} < 120 \text{ GeV}$ . If $B(t \rightarrow bH^+) \gtrsim 0.6$ , $m_{H^\pm}$ up to 160 GeV.
ABBOTT 99E	$\tan\beta \lesssim 1$ , $120 \gtrsim m_{H^\pm} > 50 \text{ GeV}$ . For $\tan\beta \gtrsim 40$ , $160 \gtrsim m_{H^\pm} > 50 \text{ GeV}$ .
ACKERSTAFF 99D	For 2DHM, only on doublet couples to lepton, $m_{H^\pm} > 0.97 \tan\beta \text{ GeV}$ 95% CL.
ACCIARRI 97F	$m_{H^\pm} > 2.6 \tan\beta \text{ GeV}$ 90% CL from excluding $B \rightarrow \tau\nu_\tau$ branching ratio.
AMMAR 97B	In low limits, $m_{H^\pm} > 0.97 \tan\beta \text{ GeV}$ 90%CL.
STAHL 97	$m_{H^\pm} > 1.5 \tan\beta \text{ GeV}$ 90% CL.
ALAM 95	The limits $m_{H^\pm} > 244 + 63/\tan\beta^{1.3}$ in the 2DHM. Light supersymmetry can invalidate this bounds.
BUSKULIC 95	$m_{H^\pm} > 1.9 \tan\beta \text{ GeV}$ 90%CL in type II.

<sup>a</sup>The data is revealed in *Particle Data Group*.

source to modify angular power spectrum. Background angular distribution on CMB experiments shows us that our universe is not perfect isotropic. There is a preferred direction imposed on background field and it produces a temperature non-uniformed distribution. On this process, we can get an incident to produce scalar particle by high energy gamma ray annihilation. Scalar particle on the cosmological potential  $V(\phi)$  is a source to induce inflation effects. On the magnetic field and electric field background, by considering their stored energy, noncommutative electroweak model can generate a theoretic clue to drive a  $V - H^0 - H^0$  coupling and produce a triple gauge boson coupling. The simulation results in a defined source higher than  $e^+e^-$  linear collider at

almost one order magnitude. It is experiment data to consider Higgs particle production and the existence opportunity of inflaton particle.

Using Feymann rule, Fig.(1), the amplitude is written as a process contains  $\gamma$  and  $Z$  resonance,

$$M_{\gamma\gamma \rightarrow H_0 H_0} = -\frac{i}{s} G_{\gamma\gamma\gamma} G_{H_0 H_0 \gamma} - \frac{i}{s - m_{H_0}^2 - im_Z \Gamma_Z} G_{\gamma\gamma Z} G_{H_0 H_0 Z} \quad (21)$$

where

$$G_{\gamma\gamma\gamma} G_{H_0 H_0 \gamma} = G_{\gamma\gamma\gamma_L} G_{H_0 H_0 \gamma_R} + G_{\gamma\gamma\gamma_R} G_{H_0 H_0 \gamma_L} \\ G_{\gamma\gamma Z} G_{H_0 H_0 Z} = G_{\gamma\gamma Z_L} G_{H_0 H_0 Z_R} + G_{\gamma\gamma Z_R} G_{H_0 H_0 Z_L} \quad (22)$$

the couplings  $G_{\gamma\gamma\gamma,Z}$  and  $G_{H_0H_0\gamma,Z}$  are the triple gauge boson helicity product,  $\Gamma_Z$  is  $Z$  total decay width  $\approx .24952 \pm 0.0023 GeV$ , and two Higgs to polarized gauge boson coupling respectively.

$$\begin{aligned} G_{H_0H_0\gamma} &= -ie \frac{\sqrt{s}}{2} (2(\vec{p}_1 \cdot \vec{\epsilon}_3)(\vec{p}_1 \cdot \vec{E} - m_H^2(\vec{E} \cdot \vec{\epsilon}_3)) \\ G_{H_0H_0Z} &= -ie \frac{\sqrt{s}}{4} (3 \tan \theta_w - \cot \theta_w) \\ &\quad (2(\vec{p}_1 \cdot \vec{\epsilon}_3)(\vec{p}_1 \cdot \vec{E}) - m_H^2(\vec{E} \cdot \vec{\epsilon}_3)) \end{aligned} \quad (23)$$

and

$$\begin{aligned} G_{\gamma\gamma\gamma} &= \\ 2e \sin \theta_w K_{\gamma\gamma\gamma} \left(\frac{s}{2}\right) &[(\epsilon_2 \cdot \epsilon_3)((a-1)\epsilon_1\theta k_1 + 2\epsilon_1\theta k_2)) \\ &+ (\epsilon_1 \cdot \epsilon_3)((a-1)\epsilon_2\theta k_2 + 2\epsilon_2\theta k_1)) + (a-1)(\epsilon_3\theta k_3)(\epsilon_1\epsilon_2)] \\ G_{\gamma\gamma Z} &= \\ -2e \sin \theta_w K_{\gamma\gamma Z} \left(\frac{s}{2}\right) &[(\epsilon_2 \cdot \epsilon_3)((a-1)\epsilon_1\theta k_1 + 2\epsilon_1\theta k_2)) \\ &+ (\epsilon_1 \cdot \epsilon_3)((a-1)\epsilon_2\theta k_2 + 2\epsilon_2\theta k_1)) + (a-1)(\epsilon_3\theta k_3)(\epsilon_1\epsilon_2)] \end{aligned} \quad (24)$$

where the parameter "a" is denoted as renormalization constant and  $k_3^\mu = k_1^\mu + k_2^\mu$ , and  $s = (k_1 + k_2)^2$ . Renormalization condition requires  $a = 3$ . Parity is conserved on the amplitude after exchanging photon polarization  $\vec{\epsilon}_1 \rightarrow \vec{\epsilon}_2$  and momentum  $\vec{k}_1 \rightarrow \vec{k}_2$  simultaneously.

In Eq.(11), the measurement of photon energy power spectrum is in the range from the upper bounds to the lower limits  $\frac{4m_{H_0}^2}{E_{CM}^2 y}$ .

$$\begin{aligned} \sigma(\Omega) &= \\ \int_{-x_m}^{x_m} \int_{4m_{H_0}^2/E_{CM}^2}^{x_m} &dx dy f(x) f(y) \left( \frac{1 + \xi(x)\xi(y)}{2} \right) \sigma \end{aligned} \quad (25)$$

In Fig.(3) and Fig.(4), the ratio of polarized and unpolarized cross section are sensitive to be changed on different polarized laser beam. The transverse and linear incident laser photon both are generated on the photon collider technique [1]. In the common standard model analysis, the P-even particle couples to linear polarized photon with the maximal strength to parallel polarization vector. The P-odd particle is perpendicular to the photon polarization. The neutral Higgs particle,  $H^0$ , and  $h^0$  are  $0^{++}$  quantum number in non-fermion field model, and the  $0^{++}$  and  $0^{--}$  state for the model taking fermion field into considering. The existence of  $P$  odd and  $C$  odd state results from fermion sector violates parity and charge conservation on one loop order chiral triangle diagram, anomaly magnetic moment and electric dipole moment.

In the  $\theta$  deformed spacetime, the background magnetic field will couple to polarized photon intrinsic property. We extract the background electric and magnetic products,  $\epsilon_\mu^{1,2}\theta^{\mu\nu}k_\nu^3$ ,  $\epsilon_\mu^{1,2}\theta^{\mu\nu}k_\nu^2$ , and  $\epsilon_\mu^2\theta^{\mu\nu}k_\nu^1$ , from the coupling, Eq.(18), and Eq.(19), and the momentum couples to background field by the,  $\vec{p}_{1,2} \cdot \vec{E}$ , term. The volume for the  $\vec{B} \cdot (k_i \times \epsilon_{i,j})$  production is such as momentum and circle polarization rotated around background

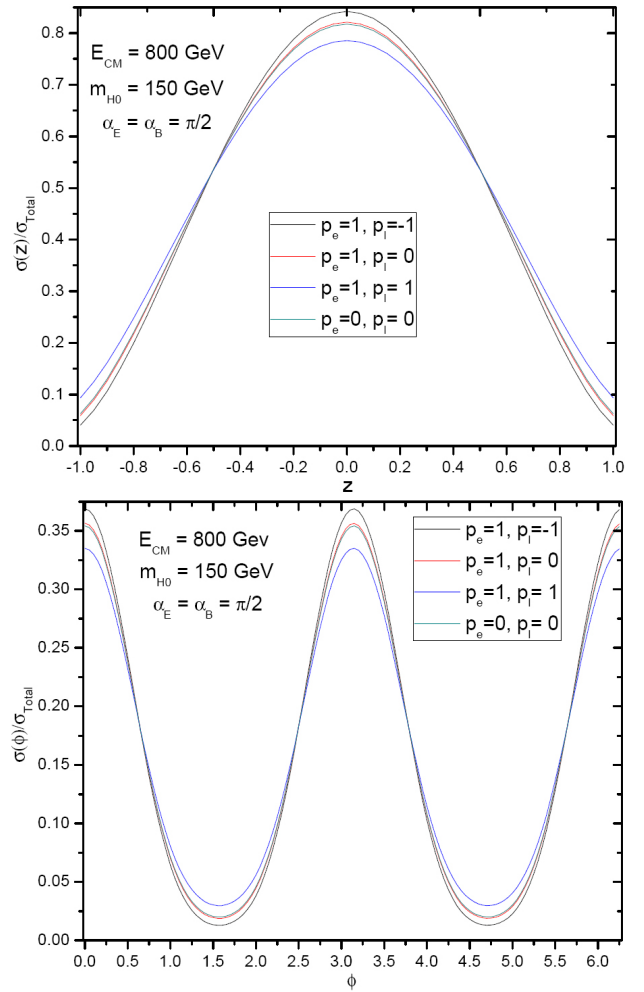


FIG. 4: The differential cross section on the energy level  $\Lambda_c = 1$  TeV, and the central energy  $E_c = 800$  GeV with Higgs mass  $m_{H_0} = 150$  GeV, the distribution at the point  $z = 0$  and at  $\phi = 0$ , the probability of differential cross section is in the maximum.

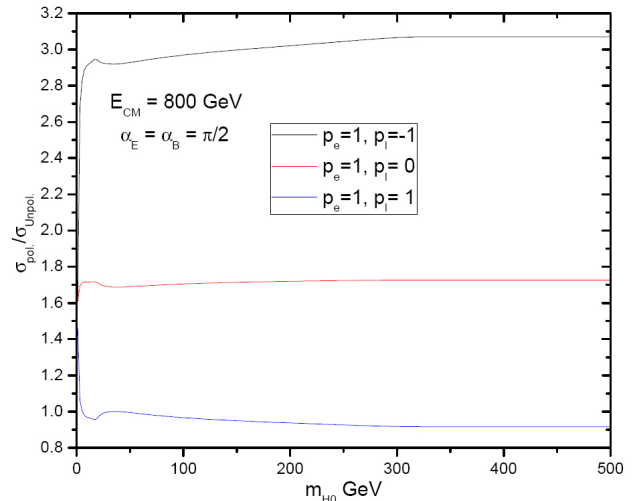


FIG. 5: The total cross section with the direction of background magnetic field, on the point of  $\alpha = \frac{\pi}{2}$  under the zero total angular momentum process, there is no parity violation evidence, and the maximum strength distribution is on the pole  $p_e = 1$  and  $p_l = -1$

$\vec{B}$  field, the electric field is similar devoted on altering momentum translational invariance.

In Fig.(5), the range for neutral Higgs particle,  $H^0$ , the mass spectrum on the maximum mode,  $p_e = 1$  and  $p_l = -1$ , will generate a maximum analysis results. The integration is restricted on getting a positive final particle velocity  $v$ . Integrating out the full x-beam channel and y-beam channel energy range<sup>2</sup>, the polarized mode and unpolarized consequence is manifestly presented. In the two sides incoming laser site, if the field direction is paralleled to the z-axis, the distribution is minimum contributed. By theoretical prediction, in the massless region particle cannot correct power distribution on its mass spectrum. The total devotion is attributed to the polarized photon gas. The coupling in Fig.(1) is  $CP$  conserved, but, violates  $C$  and  $P$  respectively by including fermion field. Without fermion field in model building,  $C$  and  $P$  can be violated or conserved respectively in  $Z$  gauge particle (see Tab.II).

We focus on  $\alpha_B = \alpha_E = \frac{\pi}{2}$  and set  $\beta_B = \beta_E = 0$ , even though the dramatic field is mainly to influence the process, but no parity effect will be generated under the field interaction with photon polarization. Intuitively, if no P-violation effect on the first order  $\theta$  deformed term, each helicity state will be equally dedicated to the process.

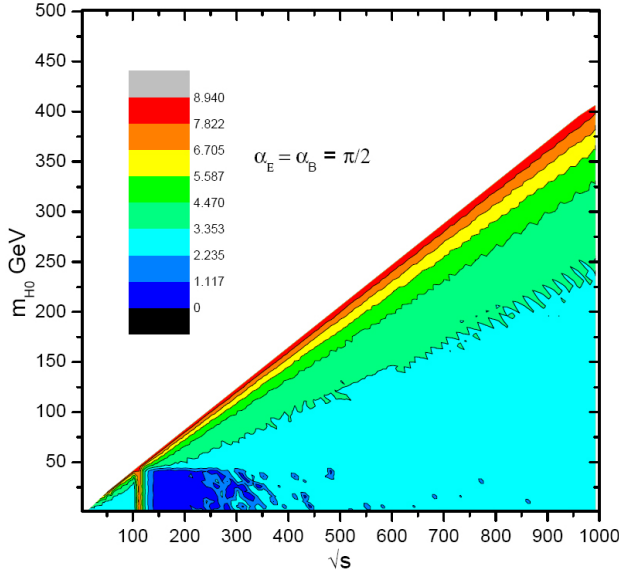


FIG. 6: The fractional power rate in the pole,  $p_e = 1$  and  $p_l = -1$ , a sensitive changing is in the central energy region  $100 \text{ GeV} \sim 500 \text{ GeV}$ . The Higgs particle mass is cutting on the  $110 \text{ GeV}$  in Tab.III, it maybe not a affective effects on the experiments detecting.

The total strength is a function as to the direction of background field  $\alpha_B$  and  $\alpha_E$ , between observer and background field direction. In Fig.(5), the total cross section is sensitive influenced by photon and electron beam. Furthermore, the incoming electron polarization

and laser photon beams will mainly control the pure laser photon. In the case,  $p_e = 1$  and  $p_l = -1$ , it is maximum power distribution on the incident point (IP). The electron and incoming laser photon are the same angular moment eigenstate. By comparing to the minimum case,  $p_e = 0$  and  $p_l = 0$ . The ratio of polarized and unpolarized beam, Fig.(6), the power distribution is minimum in the central energy between  $100 \text{ GeV} \sim 500 \text{ GeV}$ . In the region of power collapse, the massless or light particle creation is possible. The neutrino mass production in fourth generation [26, 27], it is devoted by coupling to Higgs field. The sensitive phenomena in collider physics, Fig.(6), induces a lower power distribution in lower energy domain. The linearized slope rate is increased as  $m_{H^0}$  graded. In the bounds, central energy larger than  $2m_{H^0}$ , the required power is maximum devoted on creating  $H^0$  particle.

## B. $\gamma\gamma \rightarrow H^+H^-$

In this and next section, we compare  $\gamma\gamma \rightarrow H^+H^-$  and  $H^0A^0$  with  $H^0H^0$  process. The 2HDM [6, 7, 8, 9] considers two complex scalar field on the different vacuum  $v_1$  and  $v_2$  by phase  $\xi$  connection with each other. In non-supersymmetric model, the expression of doublet scalars on its vacuum are all down type form,

$$\phi_1 = \begin{pmatrix} 0 \\ v_1 \end{pmatrix}, \quad \phi_2 = \begin{pmatrix} 0 \\ v_2 e^{i\xi} \end{pmatrix}, \quad (26)$$

by considering the general potential whether  $CP$  is conserved or not. Rotating the field into neutral  $H^0$  field and the orthogonal state goldstone field  $G^0$ , the standard massive Higgs particle is generated in the model building. Charged scalar Higgs and charged goldstone field are  $H^{+,-}$  and  $G^{+,-}$ , and the other neutral fields  $A^0$  and  $h^0$ , those are produced by imaginary part and real part. The down type doublet scale are also taking into account. There are  $CP$  even particles,  $H^{+,-}$ ,  $H^0$ , and  $h^0$ , and  $CP$  odd particle  $A^0$  in this model. The mass term for the neutral Higgs and the  $CP$  even chargeless scalar  $h^0$  are in order to diagonalize the mass mixing matrix with the rotation angle  $\alpha$  in the ground eigenstate fluctuation  $Re\phi_1$  and  $Re\phi_2$ . The only associated relation between two vacuum  $v_1$  and  $v_2$  is  $\tan\beta = \frac{v_2}{v_1}$ .

In this paper we set the  $\cos(\beta - \alpha) \ll \sin(\beta - \alpha)$ . The diagram for  $A^0h^0$  case is proportional to the  $A^0H^0$  by the factor  $\tan^2(\beta - \alpha)$ . The data in *Particle Data Group* shows that the ratio  $\tan\beta$  in the detection ABBOTT 99E<sup>3</sup> is separated by the two region,  $\tan\beta \lesssim 1$ ,  $50 < m_{H^+}(\text{GeV}) \lesssim 120$ , and  $\tan\beta \gtrsim 50$ , as  $50 < m_{H^+}(\text{GeV}) \lesssim 160$ . In the ABZOOV 02B<sup>4</sup>. For  $m_{H^+} = 75 \text{ GeV}$ , the region  $\tan\beta > 32.0$  is excluded at

<sup>2</sup> The minimal and maximum range are  $\sqrt{1 - 4m_{H^0}^2/E_{CM}^2}xy$  and  $x_m$  respectively.

<sup>3</sup> ABBOTT 99E search for a charged Higgs boson in top decays in  $p\bar{p}$  collisions at  $E_{CM} = 1.8 \text{ TeV}$ , by comparing the observed  $t\bar{t}$  cross section by assuming the the dominant decay  $t \rightarrow bW^+$  with theoretical expectation.

<sup>4</sup> ABZOOV 02B search for a charged Higgs boson in top decays with  $H^+ \rightarrow \tau^+\nu$  at central energy,  $E_{CM} = 1.8 \text{ TeV}$

90%CL. For  $\tan\beta$  values above 140, the excluded mass region extends to over 140 GeV scale. In AFFOLDER 001<sup>5</sup>, the excluded mass region extends to over 120 GeV for  $\tan\beta$  values above 100 and  $B(\tau\nu) = 1$ . By assuming the mixing angle  $\alpha$  is small, the dominated area towards into searching the fractional rate  $\tan\beta$  (see Tab.III).

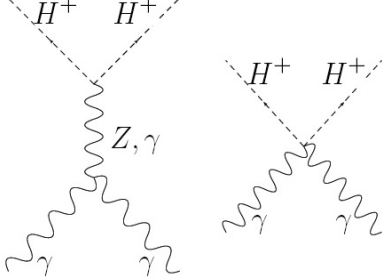


FIG. 7:  $\gamma\gamma \rightarrow Z, \gamma \rightarrow H^+H^-$

We assume charged Higgs mass  $m_{H^\pm} = 150$  GeV at  $E_{CM} = 800$  GeV. The diagram in Fig.(7) contains middle  $Z$  and  $\gamma$  resonance. Neutral Higgs production in noncommutative model, the coupling is derived by Fig.(1). In the loop calculation, the effective lagrangian, the standard model prediction on the  $\phi^0 \rightarrow \gamma\gamma$  couplings<sup>6</sup> is sensitively dependent on Higgs mass. This program is a standard process working on noncommutative triple gauge boson coupling  $\gamma\gamma Z^0$  and  $\gamma\gamma\gamma$ , and standard model,  $Z^0 H^+ H^-$ , predicted one. The coupling between photon helicity polarization to background field,  $H^+ H^-$  pairs gets a minimum by comparing to  $H^0 H^0$  and  $A^0 H^0$  processes.

The amplitude on the gamma ray helicity state is contributed by first order  $\theta$  deformed term. It appears that the total cross section is single two order deformation. The order magnitude around the electroweak scale is approaching to  $\frac{s}{\Lambda_C^2}$  extension.

$$\begin{aligned}
 M_{\gamma\gamma \rightarrow H^+H^-} = & \\
 & 2 \left( \frac{k_{\gamma\gamma Z} \cos 2\theta_W}{s - m_Z^2 - im_Z \Gamma_Z} - \frac{K_{\gamma\gamma\gamma} \sin 2\theta_W}{s} \right) \\
 & \left( \square_L [p_2 \cdot \epsilon_{3R} - p_1 \cdot \epsilon_{3R}] + \square_R [p_2 \cdot \epsilon_{3L} - p_1 \cdot \epsilon_{3L}] \right. \\
 & \left. + 2i\epsilon_1 \cdot \epsilon_2 \right), \tag{28}
 \end{aligned}$$

<sup>5</sup> Searching a charged Higgs boson in top decays with the  $H^+ \rightarrow \tau^+ \nu$  in hadron collider  $p\bar{p}$  at  $E_{CM} = 1.8$  TeV.

<sup>6</sup> The loop diagrams contain chargeless particle and charged particle.

$$\mathcal{L}_{int} = -\frac{gm_f}{2m_W} \bar{\psi}\psi\phi^0 + gm_W W_\mu^+ W^{\mu-} \phi^0 - \frac{gm_H^2}{m_W} H^+ H^- \phi^0 + \dots \tag{27}$$

The deviation for spin-1, spin-0, and spin- $\frac{1}{2}$  middle states that bosonic symmetry is violated on the one loop level.

in which

$$\begin{aligned}
 \square_i = & (a-1) \left( \frac{s}{2} \right) (\epsilon_1 \cdot \epsilon_2) (\epsilon_{3i} \theta k_3) \\
 & + \left( \frac{s}{2} \right) ((a-1)\epsilon_1 \theta k_1 - 2\epsilon_1 \theta k_2) \epsilon_2 \cdot \epsilon_{3i} \\
 & + \left( \frac{s}{2} \right) ((a-1)\epsilon_2 \theta k_2 - 2\epsilon_2 \theta k_1) \epsilon_1 \cdot \epsilon_{3i}, \tag{29}
 \end{aligned}$$

the index  $i$  denotes right-handed and left-handed circular polarization. In order to avoid considering the change of the interaction between background field and the mediated gauge boson. We contract the gauge boson polarization with the coupling tensor immediately. Extracting separated terms, Eq.(22) shows that the couples between particle momentum and gauge boson polarization on the content is an important role to decide the physical results. The integration of energy fractional rate upper and lower limits are

$$\begin{aligned}
 \sigma(\Omega) = & \\
 & \int_0^{x_m} \int_{4m_{H^\pm}^2/E_{CM}^2}^{x_m} dx dy f(x) f(y) \left( \frac{1 + \xi(x)\xi(y)}{2} \right) \sigma, \tag{30}
 \end{aligned}$$

the range should be up to  $x_m$  threshold ratio and down to the particle creation condition, the particle velocity has to be  $\geq 0$  at least. The  $Z$  resonance cannot take a constraint on energy range from lower than  $m_Z$  to the TeV scale. The photon power spectrum is a function restricted into the region, lower bound is under the causality constraint and upper limits is lower the machine maximum power restrictions.

In the photon photon backreact collider technology, the total cross section is associated with incoming laser energy rate, and constrained by the physical quantity. The parameter in this process is background field direction,  $\vec{B}$ , and  $\vec{E}$ , and the scalar mass under the assumption of the perturbation scale,  $\Lambda_C$ , is around 1TeV. We set  $\beta_B = \beta_E = 0$ , and the central energy,  $E_{CM}$ , at 800 GeV. The total cross section is dependent on  $\alpha_B$  and  $\alpha_E$  parameters. This is an abnormal imposed variables, due to background field influence.

The globe angle,  $\Omega$ , is similar as a variables of the probability of charged Higgs boson creating process. In incoming photon and electron beam, the polarization sensitively controls the experiments consequence. The dominant contribution is on  $p_e = 1$  and  $p_l = -1$  mode polarized pole. The maximum polarized value in Fig.(8) is around 0.5018 in first figure and 0.177 in second figure. The background field is playing a ridicule role on the total cross section. In the globe consequence, the angle  $\alpha_E$  and  $\alpha_B$ , and  $\beta_E$  and  $\beta_B$  are existed in the experiments parameters. They are independent with the detector direction. Naturally, the distribution cannot be shifted by moving to different site. The pole  $p_e = 1$ ,  $p_l = -1$  is a maximum contribution, the pole  $p_e = 1$ ,  $p_l = 1$  produce a minimum deviation on the final results. We set  $\alpha_E = \alpha_B = \frac{\pi}{2}$ , and  $\beta_E = \beta_B = 0$  on the  $\gamma Z$  channel.

The mass spectrum in Fig.(9) is very different as taking  $m_{H^\pm} = 0$ . It results from the high frequency pho-

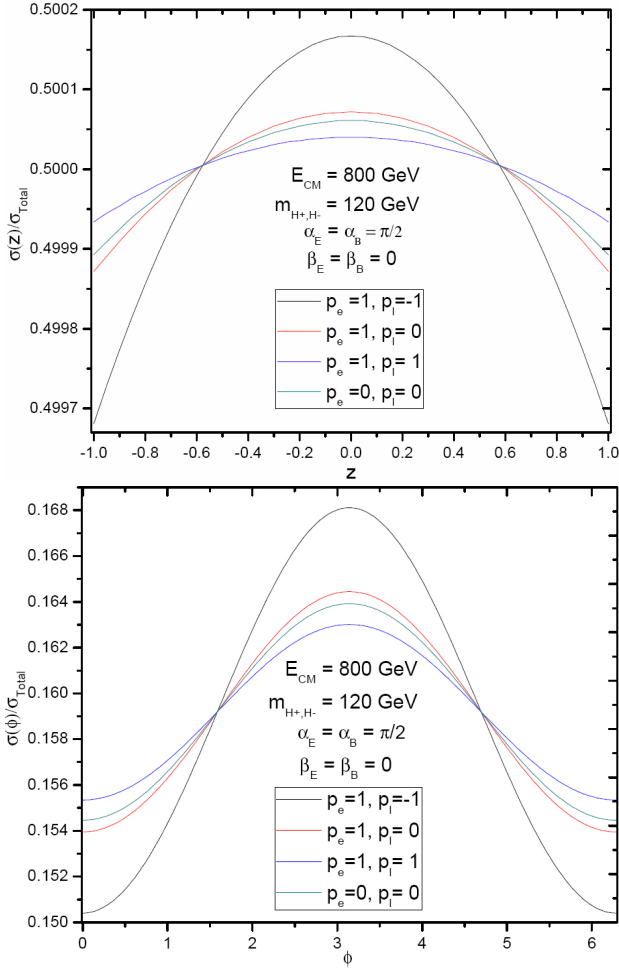


FIG. 8: The differential cross section in the energy level  $\Lambda_c = 1\text{TeV}$ , and the central energy  $E_c = 800$  GeV with Higgs mass  $m_{H^\pm} = 120$  GeV. The distribution on the point,  $z = 0$  and  $\phi = 0$ , the probability distribution is maximum distributed.

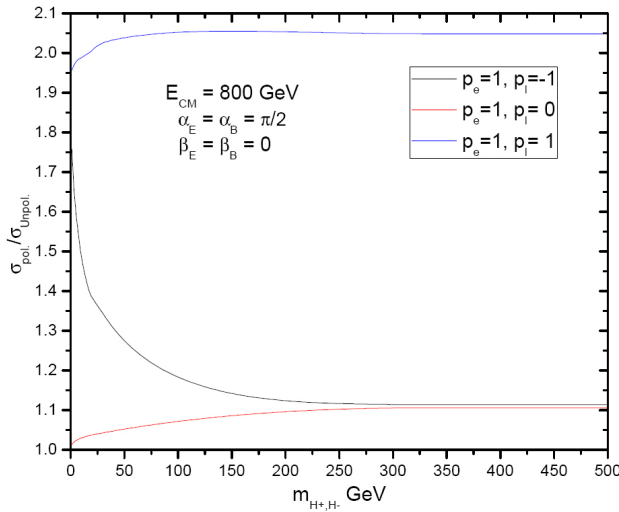


FIG. 9: The total cross section with the direction of background magnetic field, on the point of  $\alpha = \frac{\pi}{2}$  under the zero total angular momentum process, there are no parity violation evidence on the figure, the maximum strength distribution is on polarized beam of the  $p_e = 1$  and  $p_l = -1$

ton remnants. The modified energy is stored into background field interaction with photon polarization. The  $p_e = 0, p_l = 0$  pole is minimal contributed on the polarized rate. Contrastively, the pole  $p_e = 1, p_l = 1$  is maximum devoted at  $E_{\text{CM}} = 800$  GeV. This is a very dramatic phenomena in probing charged Higgs in high energy gamma ray collision. In the limit region, photon polarization  $p_l = 0$  and  $-1$  is approaching to the same rate. The maximum power fractional deviation is posed on the pole  $p_l = 1$ .

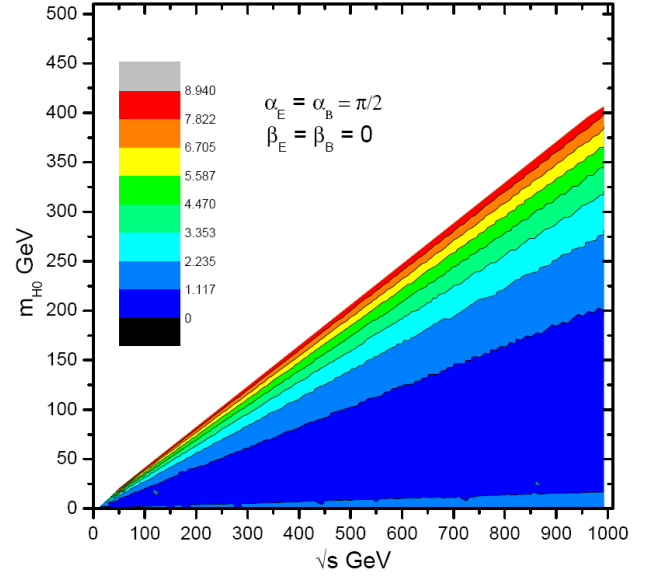


FIG. 10: The fractional power distribution is posed on  $\alpha_{E,B} = \frac{\pi}{2}$  and  $\beta_{E,B} = 0$ . The regular deviation is working on the restriction of  $E_{\text{CM}} = m_{H^\pm}$ . Near the deadline, it is maximum devoted

In the Fig.(10), it is a regular form for the process. The minimum is in the right-down corn, and the maximum is in the high slope area. Under the minimum momentum final state, particle power is maximum distributed. At the lower mass spectrum, particle is vastly numerous produced in the fine changing on central energy. In the defined background direction, it does not vary dramatically. At low energy scale to high energy scale, power spectrum is similar as the same linear function from the massless point to 400 GeV mass scale. Linear distribution in power spectrum implies that the relation between incoming high energy photon frequency is uniformed devoted on the particle angular distribution. The fractional rate in photon gas power spectrum denotes that particle mass is a smooth function with its angular distribution.

### C. $\gamma\gamma \rightarrow H^0 A^0$

By comparing neutral Higgs and charged Higgs production process, in this section we introduce a  $CPV$  scalar particle  $A^0$  in the photon photon collision background technique. The general model building, scalar potential in 2DHM is  $CP$  odd as to consider the imagine part of the factor  $\sin \xi$ . It is a  $CP$  even by ignoring the factor from the process. Splitting the complex field

$\phi_1$  and  $\phi_2$  into real part and imagine part, there are two extra degrees of freedom will be indicated into particle creation. The  $CPV$  particle  $A^0$  is induced by the imagine field, the real part produces a  $CP$  even particle  $h^0$ .

In the high energy gamma ray background creation, it contains a fluently pure high energy gamma ray simulation analysis. In Tab.II, the quantum number  $A^0$  particle is under  $0^{+-}$  state in the model without lepton and quark sector. In which  $CP$  even and  $CP$  odd melted vacuum, the  $CPV$  effects is embed into a non-equilibrium state. The  $P$  violated coupling  $ZH^0A^0$  is not a physical quality due to unitary and bosonic symmetry is inherent property in vacuum. Bosonic condition considers  $C$  and  $P$  or  $CP$  conservation.  $CPT$  preserves on the thermal equilibrium, and the conservation law imposes on  $\mathcal{L}(t)$  is same as exchanging  $t \rightarrow -t$ .  $P$  conservation is a natural effects in the  $\gamma\gamma$  to  $H^0A^0$  process. By considering the background in high frequency photon gas, the expectative influence is  $P$  violated and  $C$  violated phenomenon. In this process  $C$  violation is visible, but,  $P$  is disappeared, since, no first order  $\theta$  deformed term in the cross section with no helicity state in final created fields. The  $A^0$  mass distribution is in a region, the mass spectrum is dependent on background field direction, expansion scale, and incoming energy. In supersymmetry model, the extra  $H_1^0$  and  $H_2^0$  scalar particle is added into model by considering a up type and a down type doublet. The only unknown variables are the  $m_{A^0}$  and  $\tan\beta$  in 2DHM.

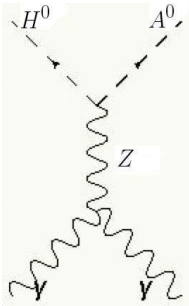


FIG. 11:  $\gamma\gamma \rightarrow H^0 A^0$

The momentum of final state particle  $H^0$  and  $A^0$  on the CM frame are  $|p_{H^0}| = |p_{A^0}| = \frac{\sqrt{s}}{2}|\vec{v}|$ , and the velocity  $|\vec{v}|$  is

$$v = \sqrt{1 + \left(\frac{m_{H^0}^2}{s} - \frac{m_{A^0}^2}{s}\right)^2 - 2\left(\frac{m_{H^0}^2}{s} + \frac{m_{A^0}^2}{s}\right)}, \quad (31)$$

the lower bound is onto the mathematics condition. Its amplitude is

$$M_{\gamma\gamma \rightarrow H^0 A^0} = -2i \frac{K_{\gamma\gamma Z}}{s - m_Z^2 - im_Z\Gamma_Z} \left( \square_L [p_2 \cdot \epsilon_{3R} - p_1 \cdot \epsilon_{3R}] + \square_R [p_2 \cdot \epsilon_{3L} - p_1 \cdot \epsilon_{3L}] \right), \quad (32)$$

where the  $\square_i$  is introduced in Eq.(27), and the  $\Gamma_Z$  is total  $Z$  decay width. The triple gauge boson coupling,

$K_{\gamma\gamma Z}$ , sets to -0.3 on the model restriction. This process is fully contributed by noncommutative spacetime geometry,  $\theta$  second order dominates this dramatic phenomenon.

$$\sigma(\Omega) = \int_{-xm}^{xm} \int_{(m_{H^0} + m_{A^0})^2 / E_{CM}^2}^{xm} dx dy f(x) f(y) \left( \frac{1 + \xi(x)\xi(y)}{2} \right) \sigma \quad (33)$$

The symmetry distribution in Fig.(12) manifestly

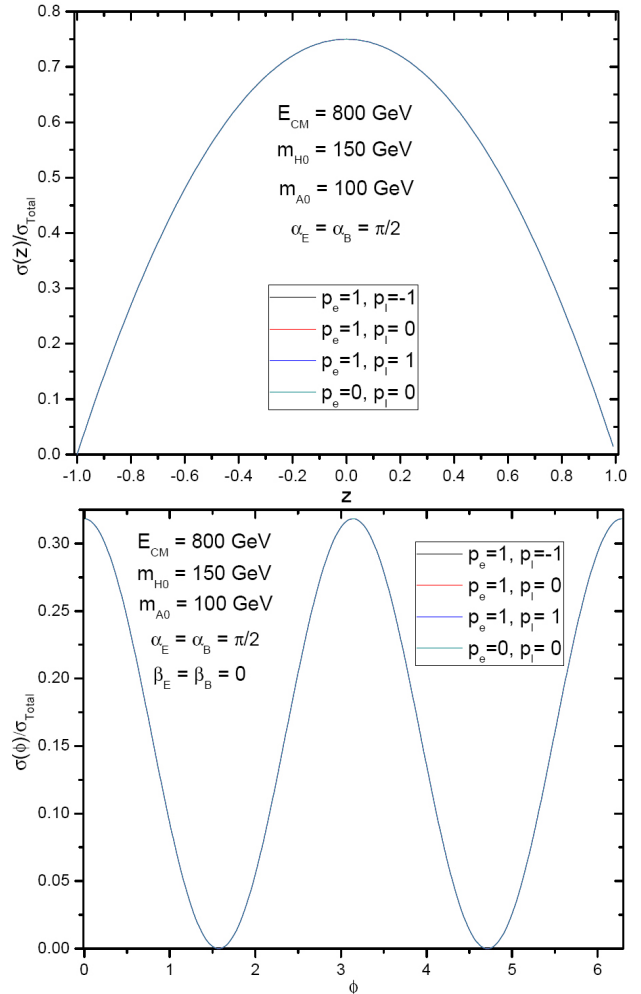


FIG. 12: The differential cross section,  $\sigma(\phi)$ , is a functional of  $\sin\alpha_{E,B}$  and  $\cos(\beta_E - \phi)$  &  $\cos(\beta_B - \phi)$ , and  $\sigma(z)$  is dependent on the  $\sin\alpha_{E,B}$ . The perturbative scale  $\Lambda_C = 1\text{TeV}$ , and the central energy  $E_C = 800$  GeV with Higgs mass  $m_{H^0} = 150$  GeV and  $m_{A^0} = 100$  GeV by imposing the background parameter  $\alpha_{E,B} = \frac{\pi}{2}$ . The contribution of all pole incoming high energy gamma ray are the same as each others.

presents the dominant distribution incident on the perpendicular to the incoming electron laser beam, it is independent on the background field direction  $\alpha_E$  or  $\alpha_B$ . The polarized rate is maximum at 7.5. The sinusoid function is associated with the background direction  $\beta_E$  and  $\beta_B$  angle. We set  $\beta_E = \beta_B = 0$  for convenient. The polarized rate is the same for all incoming laser pole, the maximum rate is 3.2 for  $m_{A^0} = 100$ , and  $m_{H^0} = 150$

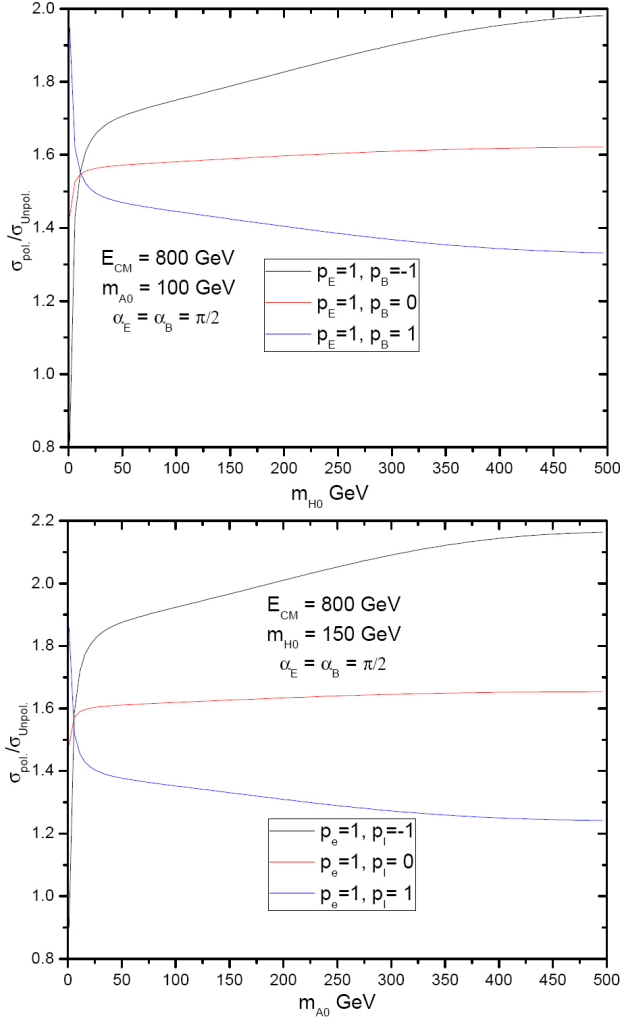


FIG. 13: The fractional power rate with the background magnetic field and electric field direction on the angle  $\alpha_E = \alpha_B = \frac{\pi}{2}$ , the maximum contribution is on the mode  $p_e = 1$ ,  $p_l = -1$ . The crossed point is around the zero mass scale, this implies that all of the scalar particles in 2DHM are as same as each other as they are massless.

The  $A^0$  and  $H^0$  mass spectrum is crossed around the 80 GeV, in Fig.(13). On the first pole, it contributes a maximum energy momentum power in backreact Compton like scattering. It shows that increasing the particle mass the fractional rate is sinuously changed. The polarized fractional rate is the same as each others as to the particle mass  $m_{H^0}$  and  $m_{A^0}$ . At the mass scale up to 500 GeV level, the maximum fractional value is around 2.2 and the minimum is down to 1.24. Formally, the incident energy at several TeV and the perturbative scale assumes at 10 TeV the final luminosity will be very small by the proportional incoming energy with scale  $\Lambda_C$ . we set the  $E_{CM}$  is 800 GeV and  $\Lambda_C$  at 1TeV level. The incident phenomenon is vivid and observed.

In the central energy  $E_{CM}$  and Higgs mass spectrum, Fig.(13) shows that the relation between central energy,  $m_{H^0}$  and  $m_{A^0}$  are similar the power range distribution at larger energy scale. It is different at the low scale power spectrum. At low photon frequency, Higgs particle,  $H^0$ , expresses a limit distribution in the

range lower than 100 GeV. The angular power deviation by  $m_{A^0}$  presents a larger density at the central energy lower than 500 GeV. The sensitive phenomenon in the photon power distribution under  $\gamma\gamma \rightarrow H^0 A^0$  process is depended on incoming high energy gamma ray. In the High frequency power range, photon photon collider presents a uniform contribution on the polarized and unpolarized event. By controlling the background field direction, there are some modifications will be emerged due to the total cross section is depended on the  $\sin^2 \alpha_{E,B}$  and  $\cos^2 \alpha_{E,B}$ .

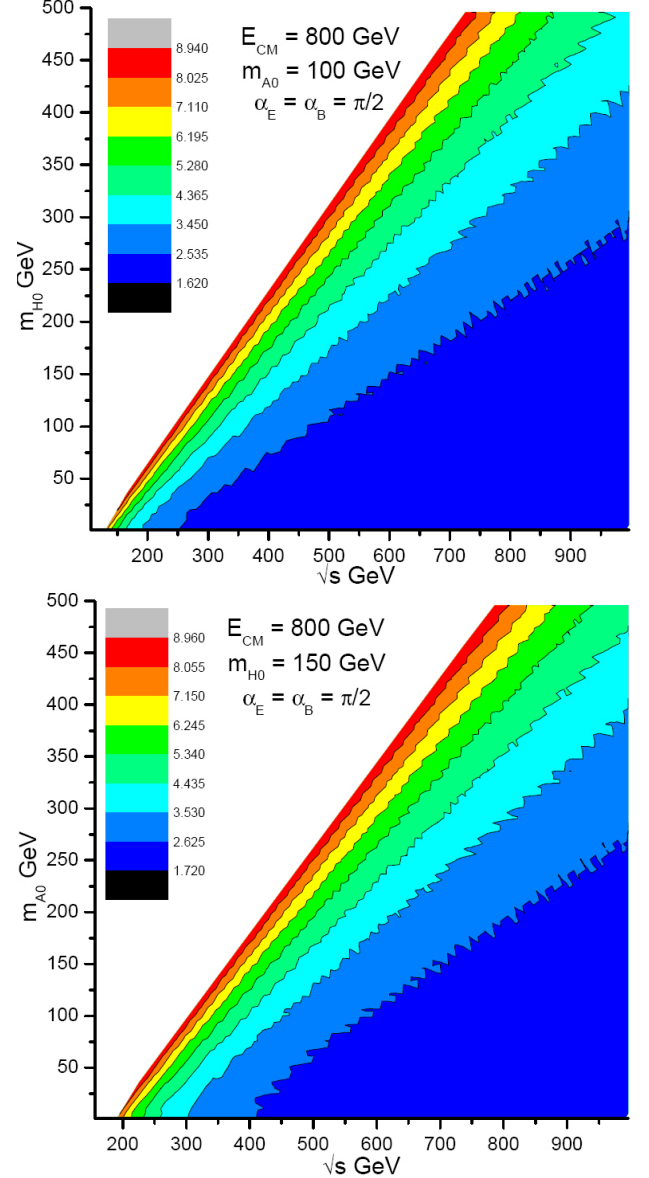


FIG. 14: The fractional rate  $\sigma_{pol.}/\sigma_{Unpol.}$  in background photon polarized mode  $p_e = 1$ ,  $p_l = -1$  and unpolarized mode  $p_e = 0$ ,  $p_l = 0$  is truncated in the line  $\sqrt{s} = m_{A^0} + m_{H^0}$ . The total cross section is dependent on the background parameters  $\sin^2 \alpha_{E,B}$ . The background field direction is  $\alpha_E = \alpha_B = \frac{\pi}{2}$ . The maximum luminosity deviation is on the border decreased as the slope descending.

From the data analysis, Fig.(14), the scalar particle mass  $m_{H^0}$  should be heavier than the mass  $m_{A^0}$ . In the lower energy of incoming photon, particle mass is pro-

duced in vacuum by high energy surroundings. In the case, the central energy in low energy range, the fractional power rate is lower distributed in the  $m_{H^0}$  mode creation than in the  $m_{A^0}$  mode. The heavier massive particle needs a higher frequency incoming laser beam in the incident point. The wave function contains tiny momentum range distribution than light particle. Below the 500 GeV central energy scale, photon power devotion in this event is dense for  $H^0$  particle, but unconsolidated for  $A^0$  particle. The probability of  $H^0$  particle creation is lower than  $A^0$  particle, thus, the mass  $m_{H^0}$  should be massive than  $m_{A^0}$ . It is a sensitive phenomena in low central energy range.

## VI. CONCLUSION

In the next order collider experiments, the most intention is to search Higgs particle. We have introduced the property of background field in photon collider technique on Higgs particle creation process in noncommutative spacetime geometry. The interesting point on the  $\gamma\gamma \rightarrow H^0 H^0$  process is the complete  $\theta$  two order deformation. It is complete forbidden by standard model prediction due to bosonic condition. Noncommutative  $\theta$  deformed spacetime slightly influences our live-world. Lorentz symmetry due to the background magnetic field and electric field violates Lorentz trans-

formation. Photon-photon collider experiment is a better candidate to test triple gauge boson coupling. In this paper, we analyse photon power distribution on the backreact scattering, the fractional rate between polarized and unpolarized pole is associated with the incoming energy and the final particle mass spectrum. The maximum devotion is manifestly dependent on the incoming photon frequency. In the last two section, we compare the  $H^0 H^0$  process with  $H^+ H^-$  and  $A^0 H^0$  one, and taking a constraint on the restriction  $m_{H^0} > m_{A^0}$ . Power law presents that the scale Higgs creation is vast and numerous by the central energy upper than the final particle produced scale. For the massless charged Higgs  $m^\pm$ , charged  $H^+$  and  $H^-$  particle are as the same field, due to charge distribution is dependent on its mass region. For the  $A^0 H^0$  case, the devotion on the fractional differential cross section in the high pole area to lower pole one, the fraction rate are all the same.

## Acknowledgments

We will thank Professor Chang for useful discuss. This work is also partially discussed with National Science Council of R.O.C. under contact: NSC-95-2112-M-007-059-MY3 and National Tsing Hua University under contact: 97N2309F1.

- 
- [1] *Photon Collider at TESLA*, <http://www.desy.de/telnov/ggtesla/#para>; I. Watanabe *et al.*, KEK Report 97-17; B. Badelek *et al.* [ECFA/DESY Photon Collider Working Group], Int. J. Mod. Phys. A **19**, 5097 (2004) [arXiv:hep-ex/0108012]. B. Badelek *et al.* [ECFA/DESY Photon Collider Working Group], Int. J. Mod. Phys. A **19**, 5097 (2004) [arXiv:hep-ex/0108012]; D. Asner, B. Grzadkowski, J. F. Gunion, H. E. Logan, V. Martin, M. Schmitt and M. M. Velasco, arXiv:hep-ph/0208219.
- [2] N. Seiberg and E. Witten, JHEP **9909**, 032 (1999) [arXiv:hep-th/9908142]; N. Seiberg, L. Susskind and N. Toumbas, JHEP **0006**, 021 (2000) [arXiv:hep-th/0005040];
- [3] D. Bazeia, T. Mariz, J. R. Nascimento, E. Passos and R. F. Ribeiro, J. Phys. A **36**, 4937 (2003) [arXiv:hep-th/0303122].
- [4] I. Mocioiu, M. Pospelov and R. Roiban, Phys. Rev. D **65**, 107702 (2002) [arXiv:hep-ph/0108136].
- [5] I. Hinchliffe and N. Kersting, Phys. Rev. D **64**, 116007 (2001) [arXiv:hep-ph/0104137].
- [6] J. F. Gunion and H. E. Haber, Nucl. Phys. B **272**, 1 (1986) [Erratum-ibid. B **402**, 567 (1993)]. J. F. Gunion and H. E. Haber, Nucl. Phys. B **278**, 449 (1986). J. F. Gunion and H. E. Haber, Nucl. Phys. B **307**, 445 (1988) [Erratum-ibid. B **402**, 569 (1993)]. J. F. Gunion and H. E. Haber, Phys. Rev. D **48**, 5109 (1993).
- [7] S. Dawson, J. F. Gunion, H. E. Haber, A. Seiden and G. L. Kane, Comments Nucl. Part. Phys. **14**, 259 (1990).
- [8] J. R. Ellis, J. F. Gunion, H. E. Haber, L. Roszkowski and F. Zwirner, Phys. Rev. D **39**, 844 (1989).
- [9] M. M. Muhlleitner, arXiv:hep-ph/0101263.
- [10] B. Melic, K. Passek-Kumericki, J. Trampetic, P. Schupp and M. Wohlgenannt, Eur. Phys. J. C **42**, 499 (2005) [arXiv:hep-ph/0503064]; B. Melic, K. Passek-Kumericki, J. Trampetic, P. Schupp and M. Wohlgenannt, Eur. Phys. J. C **42**, 483 (2005) [arXiv:hep-ph/0502249]; X. Calmet, B. Jurco, P. Schupp, J. Wess and M. Wohlgenannt, Eur. Phys. J. C **23**, 363 (2002) [arXiv:hep-ph/0111115].
- [11] A. Tureanu, arXiv:0706.0334 [hep-th]; A. P. Balachandran, A. R. Queiroz, A. M. Marques and P. Teotonio-Sobrinho, Phys. Rev. D **77**, 105032 (2008) [arXiv:0706.0021 [hep-th]]; M. Chaichian, P. P. Kulish, K. Nishijima and A. Tureanu, Phys. Lett. B **604**, 98 (2004) [arXiv:hep-th/0408069].
- [12] H. Davoudiasl, R. Kitano, G. D. Kribs, H. Murayama and P. J. Steinhardt, Phys. Rev. Lett. **93**, 201301 (2004) [arXiv:hep-ph/0403019]. N. F. Bell, B. Kayser and S. S. C. Law, arXiv:0806.3307 [hep-ph]. S. Davidson, E. Nardi and Y. Nir, arXiv:0802.2962 [hep-ph]. O. Bertolami, D. Colladay, V. A. Kostelecky and R. Potting, Phys. Lett. B **395**, 178 (1997) [arXiv:hep-ph/9612437].
- [13] M. Buric, T. Grammatikopoulos, J. Madore and G. Zoupanos, JHEP **0604**, 054 (2006) [arXiv:hep-th/0603044].
- [14] V. O. Rivelles, Phys. Lett. B **558**, 191 (2003) [arXiv:hep-th/0212262].
- [15] F. T. Brandt and M. R. Elias-Filho, Phys. Rev. D **74**, 067704 (2006) [arXiv:hep-th/0609106].
- [16] J. W. Moffat, J. Math. Phys. **36**, 3722 (1995) [Erratum-ibid. **36**, 7128 (1995)]. J. W. Moffat, arXiv:gr-qc/9605016; J. W. Moffat, arXiv:astro-ph/9704300;
- [17] N. Kersting and Y. L. Ma, arXiv:hep-ph/0305244.

- [18] K. Cheung, C. S. Kim and J. Song, Phys. Rev. D **72**, 115015 (2005) [arXiv:hep-ph/0509017]. K. Cheung, C. S. Kim and J. h. Song, Phys. Rev. D **69**, 075011 (2004) [arXiv:hep-ph/0311295].
- [19] I. Antoniadis, N. Arkani-Hamed, S. Dimopoulos and G. R. Dvali, Phys. Lett. B **436**, 257 (1998) [arXiv:hep-ph/9804398]. N. Arkani-Hamed, S. Dimopoulos and G. R. Dvali, Phys. Lett. B **429**, 263 (1998) [arXiv:hep-ph/9803315].
- [20] A. Kundu, arXiv:0806.3815 [hep-ph].
- [21] L. Randall and R. Sundrum, Phys. Rev. Lett. **83**, 3370 (1999) [arXiv:hep-ph/9905221]. L. Randall and R. Sundrum, Phys. Rev. Lett. **83**, 4690 (1999) [arXiv:hep-th/9906064].
- [22] G. R. Dvali and A. Y. Smirnov, Nucl. Phys. B **563**, 63 (1999) [arXiv:hep-ph/9904211]. A. K. Das and O. C. W. Kong, Phys. Lett. B **470**, 149 (1999) [arXiv:hep-ph/9907272]. R. N. Mohapatra, S. Nandi and A. Perez-Lorenzana, Phys. Lett. B **466**, 115 (1999) [arXiv:hep-ph/9907520]. R. Barbieri, P. Creminelli and A. Strumia, Nucl. Phys. B **585**, 28 (2000) [arXiv:hep-ph/0002199].
- [23] H. b. Cheng, Chin. Phys. Lett. **22**, 3032 (2005) [arXiv:hep-th/0410002]; K. Poppenhaeger, S. Hossenfelder, S. Hofmann and M. Bleicher, Phys. Lett. B **582**, 1 (2004) [arXiv:hep-th/0309066].
- [24] M. Frank, N. Saad and I. Turan, arXiv:0807.0443 [hep-ph].
- [25] T. Han, J. D. Lykken and R. J. Zhang, Phys. Rev. D **59**, 105006 (1999) [arXiv:hep-ph/9811350]; G. F. Giudice, R. Rattazzi and J. D. Wells, Nucl. Phys. B **544**, 3 (1999) [arXiv:hep-ph/9811291].
- [26] S. Godfrey and S. h. Zhu, arXiv:hep-ph/0405006.
- [27] K. Belotsky, D. Fargion, M. Khlopov, R. Konoplich and K. Shibaev, Phys. Rev. D **68**, 054027 (2003) [arXiv:hep-ph/0210153].